



Published in final edited form as:

Cell Tissue Res. 2012 November ; 350(2): 199–213. doi:10.1007/s00441-012-1468-7.

INTERSTITIAL CELLS IN THE PRIMATE GASTROINTESTINAL TRACT

Peter J. A. Blair, Yulia Bayguinov, Kenton M. Sanders, and Sean M. Ward

Department of Physiology & Cell Biology, University of Nevada School of Medicine, Reno, NV 89557 USA

Abstract

Kit immunohistochemistry and confocal reconstructions have provided detailed 3-dimensional images of ICC networks throughout the gastrointestinal (GI) tract. Morphological criteria have been used to establish that different classes of ICC exist within the GI tract and physiological studies showed these classes have distinct physiological roles in GI motility. Structural studies have focused predominately on rodent models and less information is available on whether similar classes of ICC exist within the GI tracts of humans or non-human primates. Using Kit immunohistochemistry and confocal imaging we examined the 3-D structure of ICC throughout the GI tract of *Cynomolgus* monkeys. Whole or flat mounts and cryostat sections were used to examine ICC networks in LES, stomach, small intestine and colon. Anti-histamine antibodies were used to distinguish ICC from mast cells in the lamina propria. Kit labeling identified complex networks of ICC populations throughout the non-human primate GI tract that have structural characteristics similar to that described for ICC populations in rodent models. ICC-MY formed anastomosing networks in the myenteric plexus region. ICC-IM were interposed between smooth muscle cells in stomach and colon and were concentrated within the deep muscular plexus (ICC-DMP) of the intestine. ICC-SEP were found in septal regions of the antrum that separated circular muscle bundles. Spindle shaped histamine⁺ mast cells were found in the lamina propria throughout the GI tract. Since similar sub-populations of ICC exist within the GI tracts of primates and rodents, the use of rodents to study the functional roles of different classes of ICC is warranted.

Keywords

ICC; ANO1; PDGFR α ⁺ cells; *Tmem16a*; mast cells; histamine

Introduction

The discovery that interstitial cells of Cajal (ICC) express the receptor tyrosine kinase, Kit and the development of antibodies against this receptor provided a valuable tool to identify these cells within the gastrointestinal (GI) tract (Burns, et al., 1996, Maeda, et al., 1992, Torihashi, et al., 1995, Ward, et al., 1994). The use of Kit immunohistochemistry and confocal microscopy allowed investigators to image the complex 3-dimensional networks

that ICC form in different regions of the gut (Sanders, 1996, Vanderwinden, 1999). Further, double-labeling experiments provided information about the relationships between ICC and several additional cell types including enteric nerves (Beckett, et al., 2002, Iba Manneschi, et al., 2004, Iino, et al., 2008, Ward, et al., 2000), macrophages (Kinoshita, et al., 2007, Mikkelsen, 2010), PDGFR α ⁺ cells (fibroblast-like cells) (Cobine, et al., 2011, Iino, et al., 2009, Kurahashi, et al., 2008, Kurahashi, et al., 2011) and smooth muscle cells (Cobine, et al., 2010). It has been established from animal models, typically rodents, that several different classes of ICC exist throughout the GI tract based on morphological criteria (Burns, et al., 1996, Komuro, et al., 1999, Rumessen, 1994, Thuneberg, 1982).

Binding and activation of Kit by its natural ligand, stem cell factor or “*steel*” factor, was found to be critical for development and maintenance of the ICC phenotype in GI muscles (Ward, et al., 1995, Ward, et al., 1994). The functional roles of different classes of ICC were clarified by blocking Kit with neutralizing antibody or by the use of rodents with mutations in *c-kit* or *steel* (Huizinga, et al., 1995, Maeda, et al., 1992, Torihashi, et al., 1995, Ward, et al., 1995, Ward, et al., 1994). At least five physiological functions have been shown to be adversely impacted when ICC are greatly reduced in number by experimental procedures, genetic deactivation of Kit, and disease processes, suggesting the following roles for these cells: (i) ICC are pacemakers and generate electrical slow waves that organize phasic contractile behavior and provide the underlying mechanism for peristalsis and segmentation (Huizinga, et al., 1995, Ordog, et al., 1999, Ward, et al., 1994), (ii) ICC provide a propagation pathway for regeneration of slow waves so that large areas of GI organs can be entrained to a dominant pacemaker rhythm (Horiguchi, et al., 2001, Sanders, et al., 1990), (iii) Intramuscular ICC (ICC-IM) mediate part of the enteric excitatory (cholinergic) and inhibitory (nitroergic) motor inputs to GI muscles (Beckett, et al., 2002, Burns, et al., 1996, Ward, et al., 2000), (iv) ICC-IM serve as stretch receptors and regulate electrical excitability of the smooth muscle/ICC syncytium and pacemaker frequency (Strege, et al., 2003, Won, et al., 2005) and (v) ICC are also thought play a role in vagal afferent signaling in the stomach (Fox, et al., 2001).

The distribution, relationships with other cell types, and functions of ICC in the GI tract have been established primarily with rodent models. It is still uncertain whether the same classes of ICC describe the full extent of these cells in each organ of the GI tract in primates. The lack of information on the 3-dimensional structure of ICC in primate tissues has arisen because many of the studies have used cryostat or paraffin sections (Bernardini, et al., 2011, Hagger, et al., 1998, Vanderwinden, et al., 1996, Yun, et al., 2010) that do not provide such information. In the present study we examined the distribution and 3-dimensional structure of Kit⁺ ICC networks throughout the GI tracts of the non-human primate, Cynomolgus monkey (*Macaca fascicularis*). A second aim was to determine whether ICC populations in the primate GI tract were immunopositive for ANO1/*Tmem16a*, a recently identified calcium activated chloride channel (CaCC) (Caputo, et al., 2008, Gomez-Pinilla, et al., 2009, Hwang, et al., 2009, Schroeder, et al., 2008, Yang, et al., 2008, Zhu, et al., 2009). Our results show remarkable conservation of anatomical localization of ICC and formation of networks of cells throughout the GI tract of Cynomolgus monkeys. The morphology of ICC provides a structural basis that could support the various physiological functions of ICC

identified in rodents. All Kit⁺ ICC populations in the primate GI tract were ANO1/*Tmem16a* immunopositive, providing an additional marker for characterizing changes in ICC populations under pathophysiological conditions and suggesting that, like in the mouse (Hwang, et al., 2009, Zhu, et al., 2009), this Ca²⁺-activated Cl⁻ conductance may be important for pacemaker activity in primate tissues.

Methods

Animals

Gastrointestinal tissues from 20 *Cynomolgus* monkeys between the ages 2–8 years (both sexes) were obtained from Charles Rivers laboratories (Sparks, Nevada, USA) and used for the described studies. The animals were maintained and the experiments performed in accordance with the National Institutes of Health Guide for the Care and Use of Laboratory Animals. Tissues were transported in pre-cooled Krebs's Ringers buffer (KRB) to the University of Nevada, Reno and fixed within 2 hours after animals were sacrificed.

Immunohistochemical studies—For immunohistochemical studies on whole mount preparations, tissues were pinned with the mucosa facing upward to the Sylgard elastomer (Dow Corning Corp., Midland, MI, USA) base of a dissecting dish containing fresh KRB and the mucosa was removed by sharp dissection. The remaining strips of tunica muscularis were stretched to 110% of the resting length and width before being immersed in fixative solution. For single labeling, tissues were fixed in 4% w/v paraformaldehyde (1 hour; room temperature). Following fixation, tissues were washed overnight in phosphate buffered saline (PBS; 0.01M, pH 7.2) and rewashed with fresh PBS the following day (4× for 1hr). Tissues were subsequently incubated in bovine serum albumin (BSA; 1%, 1 hour at room temperature) to reduce non-specific antibody binding before being incubated for 48 hours at 4°C with an antibody raised against human Kit protein (1:100 in 0.5% Triton-X 100, R&D Systems Inc., Minneapolis, MN, USA) or an antibody raised against human platelet derived growth factor receptor α (hPDGFR α , diluted 1:100 in 0.5% Triton-X 100, R&D Systems Inc., Minneapolis, MN, USA). Immunoreactivity was detected using Alexa fluor donkey anti-goat IgG antibodies (1:1000 in PBS; 1 hour, room temperature; Molecular Probes, Eugene, OR, USA). Control tissues were prepared by omitting either primary or secondary antibodies from the incubation solution. For cryostat sections, tissues were fixed in paraformaldehyde as described above prior to being dehydrated in graded sucrose solutions (5, 10, 15 and 20% w/v in PBS, 15 minutes each for 5, 10, 15% and overnight in 20%), embedded in a 1:1 mixture of 20% sucrose in PBS and Tissue Tek (Miles, Ill., USA), and rapidly frozen in liquid nitrogen-cooled 2-methylbutane. Cryostat sections (10 μ m) were cut (Leica CM3050 cryostat) and collected on Vectabond-coated slides (Vector Labs, Inc., Burlingame, CA, USA) and processed using the antibodies in a manner similar to that described above (except sections were incubated overnight in primary antibody).

As several regions of the monkey GI tract were too thick to be examined as whole mounts, they were fixed, dehydrated and frozen as described above for cryostat sections. Flat sections (100 μ m) were then cut serially through the entire mucosa and muscle layers. Tissue sections were placed in individual wells of a 24-well plate containing PBS from mucosa to

serosal side so that sections could be examined in a serial manner. These sections were then processed similar to that described for whole mount tissues.

For double labeling, tissues were fixed in either paraformaldehyde (for histamine, PGP9.5 or hPDGFR α) or acetone (30min; 4°C) (for ANO1) and processed for cryostat sectioning. Flat sections were cut through both the mucosa and muscle layers, incubated in BSA for 1 hour before being incubated the first primary antibody directed against Kit. Due to the Kit and hPDGFR α antibodies both being raised in goat we utilized a different antibody to detect Kit protein in this double label (anti-human Kit; Dako North America, Inc. Carpinteria, CA, USA). The tissue sections were subsequently washed in PBS before being incubated in the appropriate secondary antibody. After further washing the tissue was placed in the second primary antibody (ANO1, histamine, PGP9.5 or hPDGFR α). Then tissues were washed and placed in the appropriate secondary antibody. The combinations of antibodies used are detailed in Table 1. Control tissues were prepared without primary or secondary antibodies.

After washing with PBS (overnight at 4°C), whole mounts and flat and cross cryostat sections were mounted on glass slides using Aqua-Mount (Lerner Laboratories, Pittsburgh, PA, USA) before being examined with a Zeiss LSM 510 Meta confocal microscope (Zeiss, Germany) with an excitation wavelength appropriate for Alexa fluor 488 and Alexa fluor 594. Final images were constructed using Zeiss LSM 5 Image Examiner software and converted to Tiff files for final processing in Adobe Photoshop 7.0 (Adobe Co., Mountain View, CA, USA) and Corel Draw 7.0 (Corel Corp. Ontario, Canada).

Solutions

Tissues were collected in oxygenated KRB (4°C) of the following composition (mM): NaCl 118.5; KCl 4.5; MgCl₂ 1.2; NaHCO₃ 23.8; KH₂PO₄ 1.2; dextrose 11.0; CaCl₂ 2.4. The pH of the KRB was adjusted to pH 7.3 – 7.4 when saturated with 97% O₂ – 3% CO₂ at 4°C.

Results

ICC within the lower esophageal sphincter and stomach

A Kit antibody was used to examine the regional distribution and density of interstitial cells of Cajal (ICC) throughout the *tunica muscularis* of the GI tracts of Cynomolgus monkeys.

Lower esophageal sphincter—In the LES Kit immunoreactive (Kit⁺) ICC were spindle shaped with a central oval nucleus and were interspersed between muscle cells within the circular and longitudinal muscle layers. This distribution and morphology is similar to the population of cells in the LES previously referred to as intramuscular ICC (ICC-IM) (Ward, et al., 1998). The dense population of ICC-IM ran parallel to the longitudinal axis of both muscle layers. ICC at the level of the myenteric plexus (ICC-MY) were not observed in the LES (Fig. 1).

Gastric Fundus—Confocal reconstructions of whole mounts and cryostat sections of the gastric fundus revealed Kit⁺ ICC dispersed within smooth muscle fibers in both circular and longitudinal muscle layers. Typically ICC-IM within the fundus were spindle-shaped, possessed a central ovoid nucleus and had distinct tapering processes that ran parallel to the

axis of the circular and longitudinal smooth muscle fibers (Fig. 2a–d). The bi-lateral processes of ICC-IM possessed spiny protrusions along their surfaces (Fig. 2e,f), and occasionally these processes split, forming 2–3 secondary processes with extensions that contacted neighboring ICC-IM. Thus, ICC-IM formed a loose interconnecting network (Fig. 2e,f). There were often dense aggregations of ICC-IM in the circular muscle layer that appeared to connect neighboring ICC-IM. These aggregations of cells appeared to form networks within septa and around muscle bundles and may be analogous to septal ICC (ICC-SEP). ICC-MY were not observed (Fig. 2a,b), but cells from the circular and longitudinal layers transversed the myenteric plexus region into the adjacent muscle layer and then ran parallel with the muscle fibres (Fig. 2a,c). Small round and isolated Kit⁺ cells with a morphology that resembled mast cells (Nissinen and Panula, 1995) were also occasionally observed in the fundus (Fig. 2f). *Gastric Antrum*: The gastric antrum of the Cynomolgus monkey is relatively thick (1000µm) and it was therefore not possible to perform confocal reconstructions from whole mount preparations. Therefore, reconstructions were performed on serial flat sections (100 µm) cut through the *tunica muscularis*. Kit⁺ ICC were found at multiple levels in the antrum. ICC were found at greatest density between the circular and longitudinal muscle layers, within the plane of the myenteric plexus (ICC-MY; Fig. 2g,h). ICC-MY possessed numerous thin processes extending from a rounded nuclear region that branched and interconnected with processes of the same cell and processes of adjacent ICC-MY, forming a complex anastomosing network (Fig. 2h). Another population of ICC ran parallel to circular muscle fibers, and formed bands of cells with numerous interconnecting lateral projections. These ICC extended from the myenteric plexus region and appeared to lie within septa that separated the circular muscle into discrete bundles (Fig. 2i). Septal ICC (ICC-SEP) have been described previously in canine and human gastric antrums (Horiguchi, et al., 2001, Rhee, et al., 2011) and are thought to convey pacemaker activity from the myenteric plexus region deep into the circular muscle layer (Horiguchi, et al., 2001). Cells with bipolar projections (ICC-IM) were also found dispersed within the circular muscle bundles of the antrum. These cells were similar in morphology to ICC-IM of the fundus. ICC-IM were distinct from ICC-SEP: the former appeared as individual cells with a few lateral projections contacting neighboring ICC-IM (Fig 2.g,i) in comparison to the banded or rope-like appearance of ICC-SEP networks (Fig. 2h,i). ICC-IM within the longitudinal muscle layer were distributed and possessed a similar morphology as ICC-IM of the circular layer. However, ICC-IM were not observed in many sections and flat mounts of longitudinal muscle, suggesting heterogeneity in the distributions of ICC-IM in circular and longitudinal muscle layers, which is reminiscent of ICC-IM in the murine gastric antrum (Song, et al., 2005).

ICC within the small intestine

Jejunum—In the jejunum, a dense network of Kit⁺ ICC was observed within the plane of the myenteric plexus (ICC-MY; Fig. 3a–c). ICC-MY had an oval or triangular nuclear region with numerous lateral projections extending from this region of the cell and contacting the processes of neighboring ICC-MY to form an extensive 2-dimensional network (Fig. 3a–c). The ICC-MY networks were continuous over both the circular and longitudinal layer aspects of myenteric ganglia. In interganglionic regions ICC-MY formed a dense two-dimensional network of cells. ICC-IM within the circular layer of the small

intestine ran parallel to the long axis of the smooth muscle fibers and typically had fine projections interconnecting with adjacent ICC-IM and forming a loose network. ICC-IM were increased in density close near the submucosal aspect of the circular layer and around the edges of circular muscle bundles. The population of ICC-IM near the submucosa were cells within the deep muscular plexus and referred to as ICC-DMP (Fig. 3d). Projections of these cells contacted projections of adjacent ICC-DMP, forming a network (Fig. 3d). Few ICC-IM were found within the longitudinal muscle layer. These cells ran parallel to the long axis of the longitudinal muscle fibers and possessed fine projections (Fig. 3d). ICC-IM within the longitudinal muscle layer and within the bulk of the circular muscle (outside the DMP) are not apparent in the mouse (Torihashi, et al., 1995).

ICC within the colon

Inter-taenia—Kit⁺ ICC were distributed in several anatomical positions within the colonic *tunica muscularis*. The density of distribution varied between regions of taenia and in the inter-taenia areas of the colon (Fig. 4). Within the sub-serosa of inter-taenia regions, a loose, but interconnecting, population of ICC was observed (Fig. 4a,b). These ICC had a different morphology to the ICC described in the guinea-pig colon (Aranishi, et al., 2009), but since they were in the same location in the colon wall, we refer to these cells as ICC-SS. A dense anastomosing network of ICC-MY was located at the level of the myenteric plexus. Typically ICC-MY in the proximal colon had numerous processes that extended from a triangular or oval nuclear region. The processes that extended from the perinuclear region often bifurcated into multiple processes before contacting adjacent ICC-MY (Fig. 4c). Within the circular layer, ICC-IM formed a network of cells that ran parallel to the long axis of smooth muscle cells. Several processes extended from the main axis of ICC-IM and connected adjacent ICC-IM forming a loose network of cells within this muscle layer (Fig. 4d). The inter-taenia longitudinal muscle layer of the monkey colon possessed only occasional ICC-IM.

Taenia—Similar to humans, the monkey colon possesses distinct taenia along its length and therefore we sought to determine if ICC were present within these bands of longitudinal muscle. Confocal reconstructions through the taenia revealed at least two distinct populations of ICC that formed a complex network. An interconnecting network of ICC-SS was observed within the sub-serosal region. The main axis of these cells ran parallel to smooth muscle cells, and numerous lateral projections made contacts with adjacent ICC-SS, forming a network (Fig. 4e). A secondary dense population of ICC-IM was observed within the longitudinal muscle bundles of the taenia. These cells ran parallel to smooth muscle cells but had fewer lateral projections and less indication of forming ICC-to-ICC interconnections (Fig. 4f). There was also a dense network of ICC-MY between the taenia and the circular muscle layer. These cells and the network they formed were in continuity with the ICC-MY of the inter-taenia region.

ANO1/Tmem16a expression in Kit-immunopositive ICC

A microarray expression screen showed that *Tmem16a* is highly expressed in ICC vs. other cells in the tunica muscularis (Chen, et al., 2007). Immunohistochemical studies supported this observation, showing that ICC within the human and murine GI tracts selectively

express ANO1, the gene product of *Tmem16a* (Gomez-Pinilla, et al., 2009, Hwang, et al., 2009). We therefore sought to determine if Kit⁺ ICC in the monkey also express ANO1. Double labeling showed that Kit and ANO1 were co-expressed in ICC-IM and ICC-MY of gastric fundus and antrum (Fig. 5a–f). Kit⁺ ICC-MY, ICC-DMP and ICC-IM within the circular and longitudinal layers expressed ANO1 in the small intestine (Fig. 5g–i). In the colon ICC-SS, ICC-MY and ICC-SM co-expressed Kit and ANO1 (Fig. 5j–l). In the taenia there was also cellular co-localization of Kit and ANO1 in ICC-SS, ICC-MY and ICC-IM (Fig. 5m–o). The monkey *tunica muscularis* also contains numerous small rounded Kit⁺ cells with a morphology similar to that of mast cells which were not ANO1⁺. Therefore antibodies against ANO1 serve as a more selective marker for ICC than Kit antibodies in the primate GI tract.

Kit⁺ cells within the submucosa

Spindle-shaped Kit⁺ and ANO1⁻ cells were also observed within the submucosa and lamina propria of the stomach, small intestine and colon (Fig. 6). These cells were not oriented in a specific orientation but in some cases were associated with submucosal blood vessels (Fig. 6e,f). In the submucosa of the small intestine the number of spindle shaped Kit⁺ cells were less than in the stomach and colon, however a greater number of rounded Kit⁺/ANO1⁻ cells were observed in submucosa of the small intestine. Double-labeling experiments using Kit and histamine antibodies were performed to determine whether the Kit⁺ cells were mast cells. Kit and histamine were co-expressed in a sub-population of the spindle shaped cells in the stomach, small intestine and colon, suggesting that these were mast cells and not ICC (Fig. 6a–d). An additional marker, LAMP2 was also used to identify mast cells and confirmed the results obtained with histamine (not shown).

Kit⁺ cells are distinct from PDGFR α ⁺ cells in the non-human primate GI tract

Double labeling of the monkey GI tract with antibodies raised against PDGFR α and Kit revealed that PDGFR α expression is in a separate population of cells that are distinct from Kit⁺ ICC (Fig. 7a–h). PDGFR α ⁺ cells were distributed throughout the tunica muscularis in the stomach, small intestine and colon and ran parallel to the smooth muscle fibers in the respective muscle layers. PDGFR α ⁺ cells were found in the same anatomical locations and were closely apposed to Kit⁺ ICC, but immunoreactivity for the two antibodies did not overlap and could be clearly visualized as separate cell populations (Fig. 7b,d,f,h).

DISCUSSION

In the present study we observed that ICC were distributed throughout the monkey GI tract in every organ examined. ICC-MY formed elaborate anastomosing networks within the intermuscular plane between the circular and longitudinal layers in the stomach, small intestine and colon and ICC-IM were found throughout the muscle layers of the LES, stomach and colon. ICC-IM were observed at the level of the deep muscular plexus (ICC-DMP) and within the circular layer in the small intestine. The distribution of ICC was remarkably similar to that previously observed in rodents (Albertí, et al., 2007, Burns, et al., 1997, Dickens, et al., 2001, Torihashi, et al., 1997) and more recently in a 3 dimensional examination of subpopulations of Kit⁺ ICC in the human colon (Liu, et al., 2012),

suggesting that rodents are a valid model for studying the functional roles of different populations of ICC. However, one exception to this was the more complex distribution of ICC found in the colon, primarily due to the presence of taenia, which are not present in the colons of rodents. Our results also confirm that the CaCC ANO1 is expressed in all types of ICC throughout the primate GI tract. Mast cells with spindle shaped morphology were found in the submucosa of the stomach, small intestine and colon. This is an important observation because Kit⁺ cells with a similar morphology have previously been observed in other visceral organs, and have been designated as ICC rather than mast cells, based purely on their morphology (McCloskey and Gurney, 2002, McHale, et al., 2006, Pezzone, et al., 2003, Sergeant, et al., 2006).

In the gastric antrums and small intestines of rodents ICC-MY generate pacemaker activity that underlies the phasic contractile activity of these organs (Dickens, et al., 1999, Maeda, et al., 1992, Ordog, et al., 1999, Torihashi, et al., 1995, Ward, et al., 1994). The morphological distribution and formation of ICC-MY into networks in the monkey GI tract suggests a similar role for these cells in non-human primates (Hwang, et al., 2009). ICC were also observed to project from ICC-MY deep into the circular muscle layer via septae that separated the circular muscle into bundles. The projections of ICC-SEP may provide a propagation pathway, as proposed for similar populations of ICC in the dog stomach and human jejunum (Horiguchi, et al., 2007), in which slow waves are propagated actively from the ICC-MY network into the depth of the circular muscle. ICC-SEP propagation pathways may be necessary in animals with thicker muscle layers because smooth muscle cells conduct slow waves but cannot actively regenerate these events (Sanders, et al., 1990). Thus, without an active propagation pathway slow wave amplitude would decay over very short distances (<2 mm) to a point where these events would be unable to support excitation-contraction coupling.

Additional populations of ICC (ICC-IM) were interspersed between smooth muscle fibers throughout the GI tract, including the taenia. ICC-IM often contacted adjacent ICC-IM forming a loose interconnecting network. In the small intestine ICC-IM concentrated in a network adjacent to the submucosal surface of the circular layer at the level of the deep muscular plexus (ICC-DMP). However, unlike in rodents, ICC-IM were also found throughout the circular muscle layer. ICC-IM in the stomach and ICC-DMP in the small intestine have been reported to be closely apposed to enteric motor neurons and play a role in mediating cholinergic and nitrgenic neurotransmission (Beckett, et al., 2002, Burns, et al., 1996, Ward, et al., 2000). The observation that ICC-IM from both muscle layers of the stomach transversed into the adjacent muscle layer provides morphological evidence that both layers are interconnected via ICC-IM, which may provide a communication pathway for simultaneous functional responses.

The distribution of ICC in the taenia has not previously been systematically examined. In the present study we describe several classes of ICC within the monkey taenia including a population of sub-serosal cells (ICC-SS) and a dense network of ICC-IM within these bands of longitudinal muscle. The role of these cells is currently unknown and remains to be determined. Interestingly ICC-SS were also observed in non-taenia regions of the colon but their morphology differed from the ICC-SS of the taenia. Both taenia and non-taenia ICC-

SS have a different morphology to the ICC-SS previously observed in the guinea-pig colon (Aranishi, et al., 2009). Since ICC occupy the same anatomical locations in the non-human primate, it is possible that they act as intermediaries in enteric neurotransmission in primate tissues. Future examinations of the relationship between chemically identified enteric nerve fibers and ICC within the primate GI tract will determine if this is the case.

In several recent reports it has been described that ICC in the murine, monkey and human GI tract express ANO1 (AKA Dog-1) (Gomez-Pinilla, et al., 2009, Hwang, et al., 2009, Rhee, et al., 2011), a CaCC encoded by *Tmem16a* (Caputo, et al., 2008, Schroeder, et al., 2008, Yang, et al., 2008). Gastrointestinal stromal tumors (GISTs) have also been shown to express ANO1 (Espinosa, et al., 2008). In the present study we have provided further evidence that ANO1 is highly expressed in primate ICC and co-localizes at the cellular level with Kit in all classes of ICC throughout the monkey GI tract. ANO1 therefore provides a second label for ICC in the GI tract, and since antibodies against ANO1 do not label mast cells they are in fact a more specific marker (Gomez-Pinilla, et al., 2009, Hwang, et al., 2009). Isolated ICC exhibit a robust calcium activated chloride conductance (Zhu, et al., 2009), which is thought to underlie pacemaker activity as ANO1 expression in ICC was recently shown to be critical for the generation of slow waves (Hwang, et al., 2009). Expression of ANO1 in the ICC-MY of primate muscles would suggest that this CaCC also plays a role in pacemaker activity in this species. However, this hypothesis will need verification using electrophysiological experiments on isolated ICC of this species. ANO1 is expressed in spindle shaped ICC-IM in the monkey fundus, antrum and colon, and in ICC-DMP of the small intestine. Recently it has been shown that stimulation of muscarinic receptors on murine ICC-DMP results in activation of a CaCC (Zhu, et al., 2011), though further experiments will be required to confirm whether CaCCs play a similar role in neurotransmission in primates.

The distribution and 3-dimensional architecture of ICC networks and their relationships with other cell types within the *tunica muscularis* such as smooth muscle cells, neurons and resident macrophages (Beckett, et al., 2002, Ibba Manneschi, et al., 2004, Iino, et al., 2008, Kinoshita, et al., 2007, Mikkelsen, 2010, Ward, et al., 2000), was facilitated by the discovery that ICC express the receptor tyrosine kinase Kit (Burns, et al., 1996, Maeda, et al., 1992, Torihashi, et al., 1995, Ward, et al., 1994). The only other cell type that expresses Kit within the *tunica muscularis* are mast cells. Mast cells have typically been distinguished from ICC by their scattered distribution and small rounded morphology (Nissinen and Panula, 1995). We observed spindle-shaped, Kit⁺ cells in the submucosa of the primate GI tract. Double labeling with an antibody raised against histamine, reported to identify activated mast cells (Grützkau, et al., 2004, Johansson, et al., 1994, Nissinen and Panula, 1995, Silverman, et al., 2000), demonstrated that these cells were more likely to be mast cells rather than ICC. The morphology of these histamine⁺ cells were remarkably similar to Kit⁺ cells previously observed in several visceral organs including the bladder, ureter and urethra (McCloskey and Gurney, 2002, McHale, et al., 2006, Pezzone, et al., 2003, Sergeant, et al., 2006). These cells were concluded to be ICC based on their morphology. However, our finding illustrates that distinguishing mast cells from spindle shaped ICC using morphology alone is inadequate and underscores the importance of utilizing a specific mast

cell marker. Since not all of the spindle-shaped Kit⁺ cells in the submucosa were immunopositive for histamine, this would suggest that histamine expression varied and that some of the Kit⁺ cells may be activated while others not.

Finally, we examined the expression of Kit and PDGFR α throughout the monkey GI tract. PDGFR α has recently been used to identify an interstitial cell in the GI tracts of rodents (Cobine, et al., 2011, Iino, et al., 2009, Iino, et al., 2008, Kurahashi, et al., 2011) and more recently in humans (Kurahashi, et al., 2012). These cells are closely apposed to enteric motor nerves (Cobine, et al., 2011, Iino, et al., 2009, Kurahashi, et al., 2012, Kurahashi, et al., 2011) and it has been suggested that they may act as intermediaries in purine inhibitory motor neurotransmission (Kurahashi, et al., 2012, Kurahashi, et al., 2011). We show that PDGFR α ⁺ cells are closely apposed to Kit⁺ ICC throughout the GI tracts of monkeys but that these cells form a distinct class of interstitial cell.

In summary, discrete populations of ICC networks exist in different organs throughout the primate GI tract. These networks are remarkably similar to those described in rodent animal models, where it has been shown that they provide a pacemaker role and mediate enteric motor neurotransmission. The existence of these distinct populations of ICC, their anatomical location within the tunica muscularis and their expression of ANO1 suggests that ICC may provide a similar functional role in primate GI tissues that has been ascribed to them in other animal species.

Acknowledgments

This work was supported by NIH DK57236 and NIH P01 DK41315. The Morphology Core Laboratory supported by Program Project Grant, NIH P01 DK41315 and an equipment grant from the NCCR for the Zeiss LSM510 confocal microscope (1 S10 RR16871) were used for the immunohistochemical studies.

References

- Albertí E, Mikkelsen HB, Wang XY, Díaz M, Larsen JO, Huizinga JD, Jiménez M. Pacemaker activity and inhibitory neurotransmission in the colon of Ws/Ws mutant rats. *Am J Physiol Gastrointest Liver Physiol.* 2007; 292:G1499–1510. [PubMed: 17322067]
- Aranishi H, Kunisawa Y, Komuro T. Characterization of interstitial cells of Cajal in the subserosal layer of the guinea-pig colon. *Cell Tissue Res.* 2009; 335:323–329. [PubMed: 19048293]
- Beckett EA, Horiguchi K, Khoyi M, Sanders KM, Ward SM. Loss of enteric motor neurotransmission in the gastric fundus of SI/SI(d) mice. *J Physiol.* 2002; 543:871–887. [PubMed: 12231645]
- Bernardini N, Segnani C, Ippolito C, De Giorgio R, Colucci R, Faussone-Pellegrini MS, Chiarugi M, Campani D, Castagna M, Mattii L, Blandizzi C, Dolfi A. Immunohistochemical Analysis of Myenteric Ganglia and Interstitial Cells of Cajal in Ulcerative Colitis. *J Cell Mol Med.* 2011
- Burns AJ, Herbert TM, Ward SM, Sanders KM. Interstitial cells of Cajal in the guinea-pig gastrointestinal tract as revealed by c-Kit immunohistochemistry. *Cell Tissue Res.* 1997; 290:11–20. [PubMed: 9377631]
- Burns AJ, Lomax AE, Torihashi S, Sanders KM, Ward SM. Interstitial cells of Cajal mediate inhibitory neurotransmission in the stomach. *The Proceedings of the National Academy of Sciences.* 1996; 93:12008–12013.
- Caputo A, Caci E, Ferrera L, Pedemonte N, Barsanti C, Sondo E, Pfeffer U, Ravazzolo R, Zegarra-Moran O, Galletta LJ. TMEM16A, a membrane protein associated with calcium-dependent chloride channel activity. *Science.* 2008; 322:590–594. [PubMed: 18772398]

- Chen H, Ordög T, Chen J, Young DL, Bardsley MR, Redelman D, Ward SM, Sanders KM. Differential gene expression in functional classes of interstitial cells of Cajal in murine small intestine. *Physiol Genomics*. 2007; 31:492–509. [PubMed: 17895395]
- Cobine CA, Hennig GW, Bayguinov YR, Hatton WJ, Ward SM, Keef KD. Interstitial cells of Cajal in the cynomolgus monkey rectoanal region and their relationship to sympathetic and nitrergic nerves. *Am J Physiol Gastrointest Liver Physiol*. 2010; 298:G643–656. [PubMed: 20150245]
- Cobine CA, Hennig GW, Kurahashi M, Sanders KM, Ward SM, Keef KD. Relationship between interstitial cells of Cajal, fibroblast-like cells and inhibitory motor nerves in the internal anal sphincter. *Cell Tissue Res*. 2011; 344:17–30. [PubMed: 21337122]
- Dickens EJ, Edwards FR, Hirst GD. Selective knockout of intramuscular interstitial cells reveals their role in the generation of slow waves in mouse stomach. *J Physiol*. 2001; 531:827–833. [PubMed: 11251061]
- Dickens EJ, Hirst GD, Tomita T. Identification of rhythmically active cells in guinea-pig stomach. *J Physiol*. 1999; 514(Pt 2):515–531. [PubMed: 9852332]
- Espinosa I, Lee CH, Kim MK, Rouse BT, Subramanian S, Montgomery K, Varma S, Corless CL, Heinrich MC, Smith KS, Wang Z, Rubin B, Nielsen TO, Seitz RS, Ross DT, West RB, Cleary ML, van de Rijn M. A novel monoclonal antibody against DOG1 is a sensitive and specific marker for gastrointestinal stromal tumors. *Am J Surg Pathol*. 2008; 32:210–218. [PubMed: 18223323]
- Fox EA, Phillips RJ, Martinson FA, Baronowsky EA, Powley TL. C-Kit mutant mice have a selective loss of vagal intramuscular mechanoreceptors in the forestomach. *Anat Embryol (Berl)*. 2001; 204:11–26. [PubMed: 11506430]
- Gomez-Pinilla PJ, Gibbons SJ, Bardsley MR, Lorincz A, Pozo MJ, Pasricha PJ, Van de Rijn M, West RB, Sarr MG, Kendrick ML, Cima RR, Dozois EJ, Larson DW, Ordog T, Farrugia G. Anol1 is a selective marker of interstitial cells of Cajal in the human and mouse gastrointestinal tract. *Am J Physiol Gastrointest Liver Physiol*. 2009; 296:G1370–1381. [PubMed: 19372102]
- Grützkau A, Smorodchenko A, Lippert U, Kirchhof L, Artuc M, Henz BM. LAMP-1 and LAMP-2, but not LAMP-3, are reliable markers for activation-induced secretion of human mast cells. *Cytometry A*. 2004; 61:62–68. [PubMed: 15351990]
- Hagger R, Gharaie S, Finlayson C, Kumar D. Regional and transmural density of interstitial cells of Cajal in human colon and rectum. *Am J Physiol*. 1998; 275:G1309–1316. [PubMed: 9843767]
- Horiguchi K, Semple GS, Sanders KM, Ward SM. Distribution of pacemaker function through the tunica muscularis of the canine gastric antrum. *J Physiol*. 2001; 537:237–250. [PubMed: 11711577]
- Huizinga JD, Thuneberg L, Kluppel M, Malysz J, Mikkelsen HB, Bernstein A. W/kit gene required for interstitial cells of Cajal and for intestinal pacemaker activity. *Nature*. 1995; 373:347–349. [PubMed: 7530333]
- Hwang SJ, Blair PJ, Britton FC, O'Driscoll KE, Hennig G, Bayguinov YR, Rock JR, Harfe BD, Sanders KM, Ward SM. Expression of anoctamin 1/TMEM16A by interstitial cells of Cajal is fundamental for slow wave activity in gastrointestinal muscles. *J Physiol*. 2009; 587:4887–4904. [PubMed: 19687122]
- Ibba Manneschi L, Pacini S, Corsani L, Bechi P, Faussone-Pellegrini MS. Interstitial cells of Cajal in the human stomach: distribution and relationship with enteric innervation. *Histol Histopathol*. 2004; 19:1153–1164. [PubMed: 15375758]
- Iino S, Horiguchi K, Horiguchi S, Nojyo Y. c-Kit-negative fibroblast-like cells express platelet-derived growth factor receptor alpha in the murine gastrointestinal musculature. *Histochem Cell Biol*. 2009; 131:691–702. [PubMed: 19280210]
- Iino S, Horiguchi K, Nojyo Y. Interstitial cells of Cajal are innervated by nitrergic nerves and express nitric oxide-sensitive guanylate cyclase in the guinea-pig gastrointestinal tract. *Neuroscience*. 2008; 152:437–448. [PubMed: 18280665]
- Johansson O, Virtanen M, Hilliges M, Yang Q. Histamine immunohistochemistry is superior to the conventional heparin-based routine staining methodology for investigations of human skin mast cells. *Histochem J*. 1994; 26:424–430. [PubMed: 8045782]
- Kinoshita K, Horiguchi K, Fujisawa M, Kobirumaki F, Yamato S, Hori M, Ozaki H. Possible involvement of muscularis resident macrophages in impairment of interstitial cells of Cajal and

- myenteric nerve systems in rat models of TNBS-induced colitis. *Histochem Cell Biol.* 2007; 127:41–53. [PubMed: 16871386]
- Komuro T, Seki K, Horiguchi K. Ultrastructural characterization of the interstitial cells of Cajal. *Arch Histol Cytol.* 1999; 62:295–316. [PubMed: 10596941]
- Kurahashi M, Nakano Y, Hennig GW, Ward SM, Sanders KM. Platelet derived growth factor receptor α -positive cells in the tunica muscularis of human colon. *J Cell Mol Med.* 2012
- Kurahashi M, Niwa Y, Cheng J, Ohsaki Y, Fujita A, Goto H, Fujimoto T, Torihashi S. Platelet-derived growth factor signals play critical roles in differentiation of longitudinal smooth muscle cells in mouse embryonic gut. *Neurogastroenterol Motil.* 2008; 20:521–531. [PubMed: 18194151]
- Kurahashi M, Zheng H, Dwyer L, Ward SM, Don Koh S, Sanders KM. A functional role for the ‘fibroblast-like cells’ in gastrointestinal smooth muscles. *J Physiol.* 2011; 589:697–710. [PubMed: 21173079]
- Lee HT, Hennig GW, Fleming NW, Keef KD, Spencer NJ, Ward SM, Sanders KM, Smith TK. Septal interstitial cells of Cajal conduct pacemaker activity to excite muscle bundles in human jejunum. *Gastroenterology.* 2007; 133:907–917. [PubMed: 17678922]
- Liu YA, Chung YC, Pan ST, Hou YC, Peng SJ, Pasricha PJ, Tang SC. 3-D illustration of network orientations of interstitial cells of Cajal subgroups in human colon as revealed by deep-tissue imaging with optical clearing. *Am J Physiol Gastrointest Liver Physiol.* 2012; 302:G1099–1110. [PubMed: 22421617]
- Maeda H, Yamagata A, Nishikawa S, Yoshinaga K, Kobayashi S, Nishi K. Requirement of c-kit for development of intestinal pacemaker system. *Development.* 1992; 116:369–375. [PubMed: 1283735]
- McCloskey KD, Gurney AM. Kit positive cells in the guinea pig bladder. *J Urol.* 2002; 168:832–836. [PubMed: 12131376]
- McHale NG, Hollywood MA, Sergeant GP, Shafei M, Thornbury KT, Ward SM. Organization and function of ICC in the urinary tract. *J Physiol.* 2006; 576:689–694. [PubMed: 16916908]
- Mikkelsen HB. Interstitial cells of Cajal, macrophages and mast cells in the gut musculature: morphology, distribution, spatial and possible functional interactions. *J Cell Mol Med.* 2010; 14:818–832. [PubMed: 20132411]
- Nissinen MJ, Panula P. Developmental patterns of histamine-like immunoreactivity in the mouse. *J Histochem Cytochem.* 1995; 43:211–227. [PubMed: 7822777]
- Ordog T, Ward SM, Sanders KM. Interstitial cells of cajal generate electrical slow waves in the murine stomach. *The Journal of Physiology.* 1999; 518(Pt 1):257–269. [PubMed: 10373707]
- Pezzone MA, Watkins SC, Alber SM, King WE, de Groat WC, Chancellor MB, Fraser MO. Identification of c-kit-positive cells in the mouse ureter: the interstitial cells of Cajal of the urinary tract. *Am J Physiol Renal Physiol.* 2003; 284:F925–929. [PubMed: 12540363]
- Rhee PL, Lee JY, Son HJ, Kim JJ, Rhee JC, Kim S, Koh SD, Hwang SJ, Sanders KM, Ward SM. Analysis of Pacemaker Activity in the Human Stomach. *J Physiol.* 2011
- Rumessen JJ. Identification of interstitial cells of Cajal. Significance for studies of human small intestine and colon. *Dan Med Bull.* 1994; 41:275–293. [PubMed: 7924459]
- Sanders KM. A case for interstitial cells of Cajal as pacemakers and mediators of neurotransmission in the gastrointestinal tract. *Gastroenterology.* 1996; 111:492–515. [PubMed: 8690216]
- Sanders KM, Stevens R, Burke E, Ward SW. Slow waves actively propagate at submucosal surface of circular layer in canine colon. *Am J Physiol.* 1990; 259:G258–263. [PubMed: 2382724]
- Schroeder BC, Cheng T, Jan YN, Jan LY. Expression cloning of TMEM16A as a calcium-activated chloride channel subunit. *Cell.* 2008; 134:1019–1029. [PubMed: 18805094]
- Sergeant GP, Thornbury KD, McHale NG, Hollywood MA. Interstitial cells of Cajal in the urethra. *J Cell Mol Med.* 2006; 10:280–291. [PubMed: 16796799]
- Silverman AJ, Sutherland AK, Wilhelm M, Silver R. Mast cells migrate from blood to brain. *J Neurosci.* 2000; 20:401–408. [PubMed: 10627616]
- Song G, David G, Hirst S, Sanders KM, Ward SM. Regional variation in ICC distribution, pacemaking activity and neural responses in the longitudinal muscle of the murine stomach. *J Physiol.* 2005; 564:523–540. [PubMed: 15677686]

- Strege PR, Ou Y, Sha L, Rich A, Gibbons SJ, Szurszewski JH, Sarr MG, Farrugia G. Sodium current in human intestinal interstitial cells of Cajal. *Am J Physiol Gastrointest Liver Physiol.* 2003; 285:G1111–1121. [PubMed: 12893628]
- Thuneberg L. Interstitial cells of Cajal: intestinal pacemaker cells? *Adv Anat Embryol Cell Biol.* 1982; 71:1–130. [PubMed: 7090872]
- Torihashi S, Ward SM, Nishikawa S, Nishi K, Kobayashi S, Sanders KM. c-kit-dependent development of interstitial cells and electrical activity in the murine gastrointestinal tract. *Cell and Tissue Research.* 1995; 280:97–111. [PubMed: 7538451]
- Torihashi S, Ward SM, Sanders KM. Development of c-Kit-positive cells and the onset of electrical rhythmicity in murine small intestine. *Gastroenterology.* 1997; 112:144–155. [PubMed: 8978353]
- Vanderwinden JM. Role of Interstitial Cells of Cajal and their relationship with the enteric nervous system. *Eur J Morphol.* 1999; 37:250–256. [PubMed: 10477470]
- Vanderwinden JM, Liu H, Menu R, Conreur JL, De Laet MH, Vanderhaeghen JJ. The pathology of infantile hypertrophic pyloric stenosis after healing. *J Pediatr Surg.* 1996; 31:1530–1534. [PubMed: 8943116]
- Ward SM, Beckett EA, Wang X, Baker F, Khoyi M, Sanders KM. Interstitial cells of Cajal mediate cholinergic neurotransmission from enteric motor neurons. *J Neurosci.* 2000; 20:1393–1403. [PubMed: 10662830]
- Ward SM, Burns AJ, Torihashi S, Harney SC, Sanders KM. Impaired development of interstitial cells and intestinal electrical rhythmicity in steel mutants. *Am J Physiol.* 1995; 269:C1577–1585. [PubMed: 8572188]
- Ward SM, Burns AJ, Torihashi S, Sanders KM. Mutation of the proto-oncogene c-kit blocks development of interstitial cells and electrical rhythmicity in murine intestine. *The Journal of Physiology.* 1994; 480(Pt 1):91–97. [PubMed: 7853230]
- Ward SM, Morris G, Reese L, Wang XY, Sanders KM. Interstitial cells of Cajal mediate enteric inhibitory neurotransmission in the lower esophageal and pyloric sphincters. *Gastroenterology.* 1998; 115:314–329. [PubMed: 9679037]
- Won KJ, Sanders KM, Ward SM. Interstitial cells of Cajal mediate mechanosensitive responses in the stomach. *Proc Natl Acad Sci U S A.* 2005; 102:14913–14918. [PubMed: 16204383]
- Yang YD, Cho H, Koo JY, Tak MH, Cho Y, Shim WS, Park SP, Lee J, Lee B, Kim BM, Raouf R, Shin YK, Oh U. TMEM16A confers receptor-activated calcium-dependent chloride conductance. *Nature.* 2008; 455:1210–1215. [PubMed: 18724360]
- Yun HY, Sung R, Kim YC, Choi W, Kim HS, Kim H, Lee GJ, You RY, Park SM, Yun SJ, Kim MJ, Kim WS, Song YJ, Xu WX, Lee SJ. Regional Distribution of Interstitial Cells of Cajal (ICC) in Human Stomach. *Korean J Physiol Pharmacol.* 2010; 14:317–324. [PubMed: 21165331]
- Zhu MH, Kim TW, Ro S, Yan W, Ward SM, Koh SD, Sanders KM. A Ca(2+)-activated Cl(-) conductance in interstitial cells of Cajal linked to slow wave currents and pacemaker activity. *J Physiol.* 2009; 587:4905–4918. [PubMed: 19703958]
- Zhu MH, Sung IK, Zheng H, Sung TS, Britton FC, O'Driscoll K, Koh SD, Sanders KM. Muscarinic activation of Ca2+-activated Cl- current in interstitial cells of Cajal. *J Physiol.* 2011; 589:4565–4582. [PubMed: 21768263]

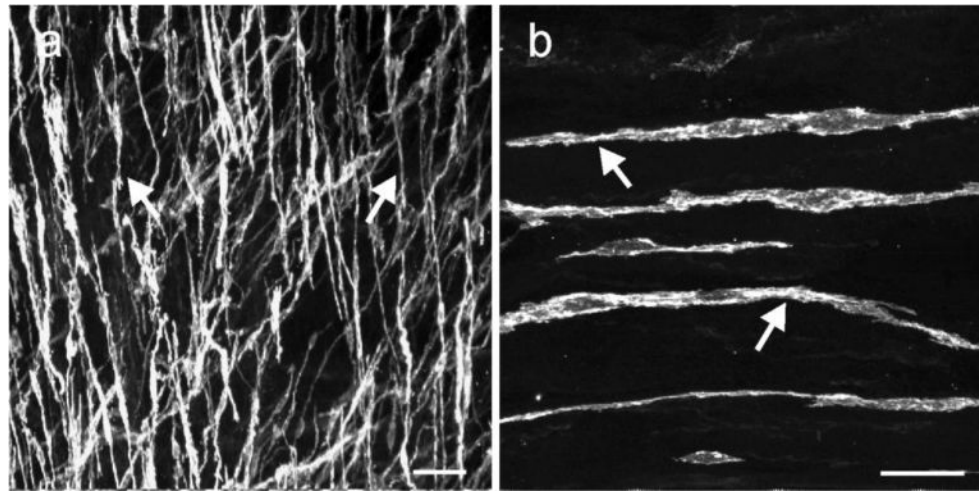


Fig. 1. ICC in the lower esophageal sphincter. **(a, b)** digital reconstructions of confocal images from flat cryosections (100 μm) of the LES. Kit^+ ICC (arrows) possessed spindle shaped morphology with a central oval nucleus and were interspersed within the circular and longitudinal muscle layers. The dense population of ICC-IM ran parallel to the longitudinal axis of the muscle fibers. Scale bars = 50 μm in **(a)** and 25 μm in **(b)**

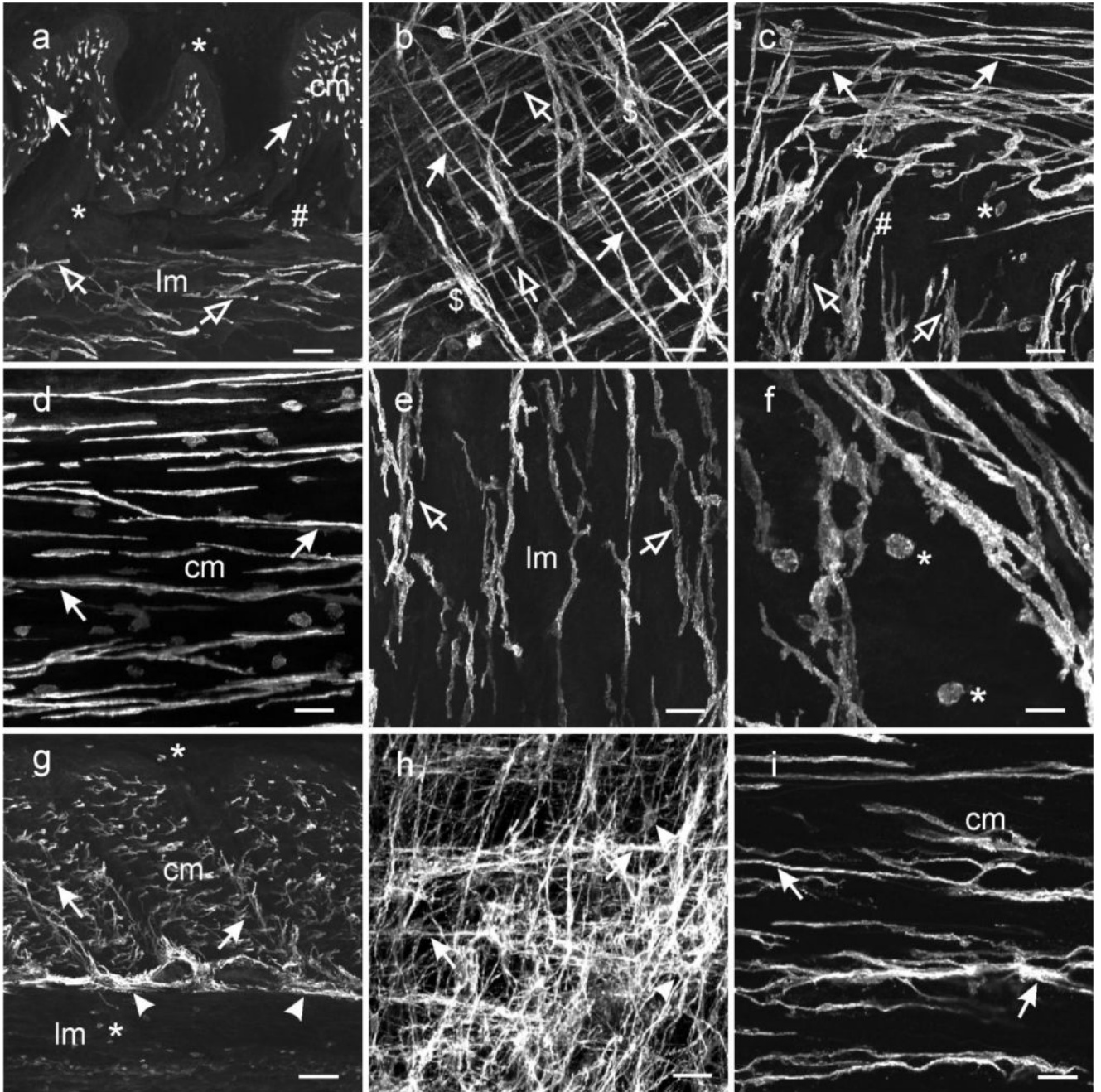


Fig. 2. Distribution of ICC in the stomach. (a–f) ICC within the gastric fundus. (a) is a cryostat cross section through the fundus wall and (b) a whole mount preparation of the fundus *tunica muscularis*. Spindle shaped Kit^+ ICC were dispersed within the circular (cm, solid arrows) and longitudinal muscle layers (lm, open arrows). The long axis of the ICC-IM cell bodies ran parallel to the smooth muscle cells of the respective muscle layers. (a,c) A distinct population of ICC was not observed adjacent to the myenteric border but ICC-IM from both muscle layers interconnected with each other and transversed both muscle layers (#). (b) Dense aggregations of ICC-IM in the circular layer (\$) appeared to form networks

within septa and around muscle bundles and may be analogous to septal ICC (ICC-SEP). **(d–e)** Not all ICC-IM in the fundus were spindle shaped **(d)** but cells in the longitudinal layer adjacent to the myenteric region **(e)** possessed several processes that often contacted adjacent ICC-IM. **(f)** At higher power, ICC-IM in both layers displayed spiny protrusions extending from the bi-lateral processes. Numerous rounded mast cells (*) were observed throughout the gastric fundus. **(g–i)** ICC within the gastric antrum. **(g)** is a cryosection cut transverse to the circular layer showing ICC-IM in the circular (cm, arrows) but not the longitudinal (lm) layer. ICC-SEP were observed to surround muscle bundles (\$). A dense network of ICC-MY were observed interspersed between and surrounding myenteric ganglia (arrowheads), that can be seen in a flat mount section **(h)**. ICC-MY possessed several processes that extended from a central nuclear region and contacted adjacent ICC-MY to form a distinct network (arrowheads). **(i)** Spindle shaped ICC-IM (arrows) ran parallel to the long axis of the circular layer (cm). ICC-IM possessed lateral processes that extended from the main body and contacted adjacent ICC-IM forming a loose network. Aggregations of ICC-IM formed rope-like networks, reminiscent of ICC-SEP (\$), within the circular layer. Numerous mast cells were observed in the longitudinal layer and along the submucosal surface of the circular layer (*). Scale bars = 100 μm in **(a & g)**, 50 μm in **(b,c,d,e,h)** and 25 μm in **(f & h)**

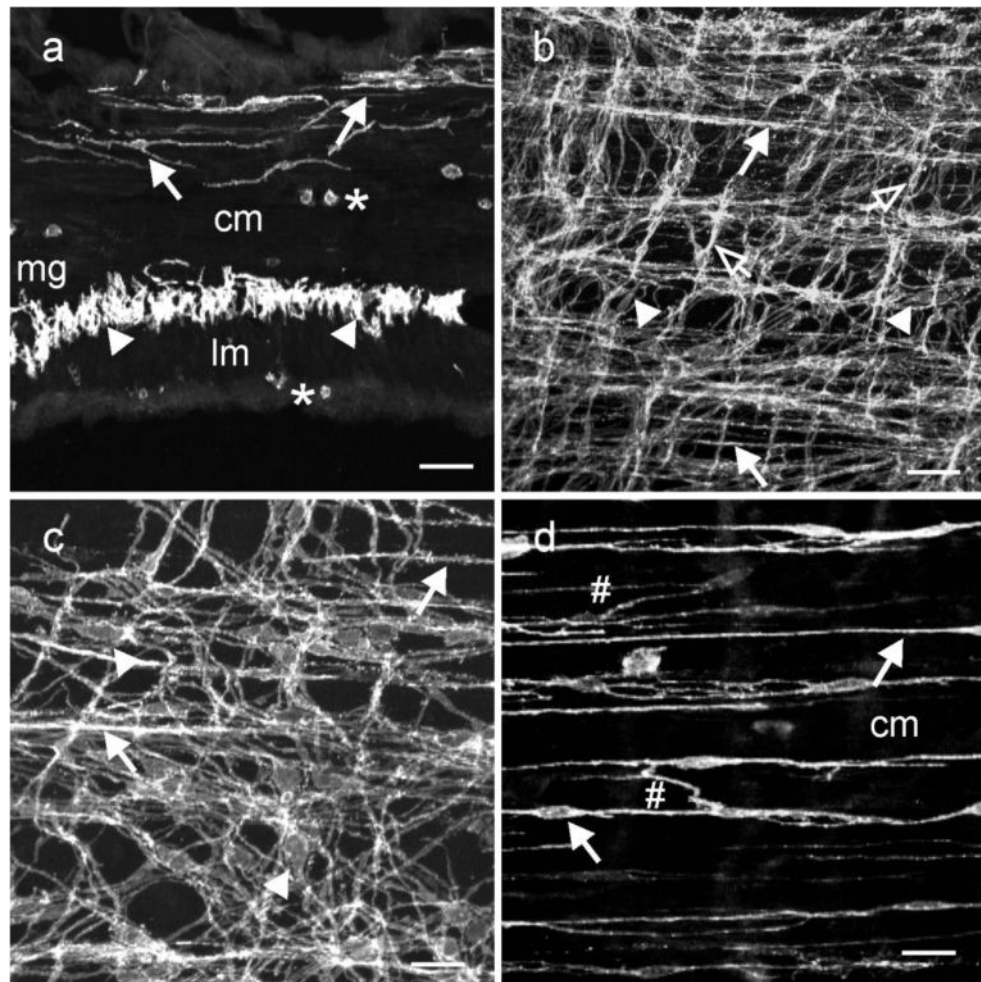


Fig. 3. ICC within the small intestine. (a) is a cryostat section cut parallel to the circular layer. ICC-IM and ICC-DMP ran parallel to the long axis of smooth muscle fibers within the circular layer (cm, solid arrows). ICC-MY (arrowheads) can be observed within the intermuscular plane between the circular and longitudinal muscle layers (Im) at the level of the myenteric plexus (mg) at higher power. Occasional mast cells (*) were observed along the serosal aspect of the Im and within the cm. (b,c) confocal reconstructions of whole mounts through the jejunum at different magnifications. A dense anastomosing network of ICC-MY was observed at the level of the myenteric plexus that formed connections with adjacent ICC-MY (arrowheads). ICC-IM were also observed along the inner aspect of the circular layer (closed arrows) and occasionally in the longitudinal layer (open arrows). (d) is a digital reconstruction of ICC-IM through the circular layer. ICC-DMP were observed on the inner aspect of the circular layer (arrows) and ICC-IM were observed within the circular layer. ICC-DMP and ICC-IM possessed lateral projections that formed a loose interconnecting network with other ICC-IM (#;d). Scale bars = 50 μ m in (d & b) and 25 μ m in (c & d)

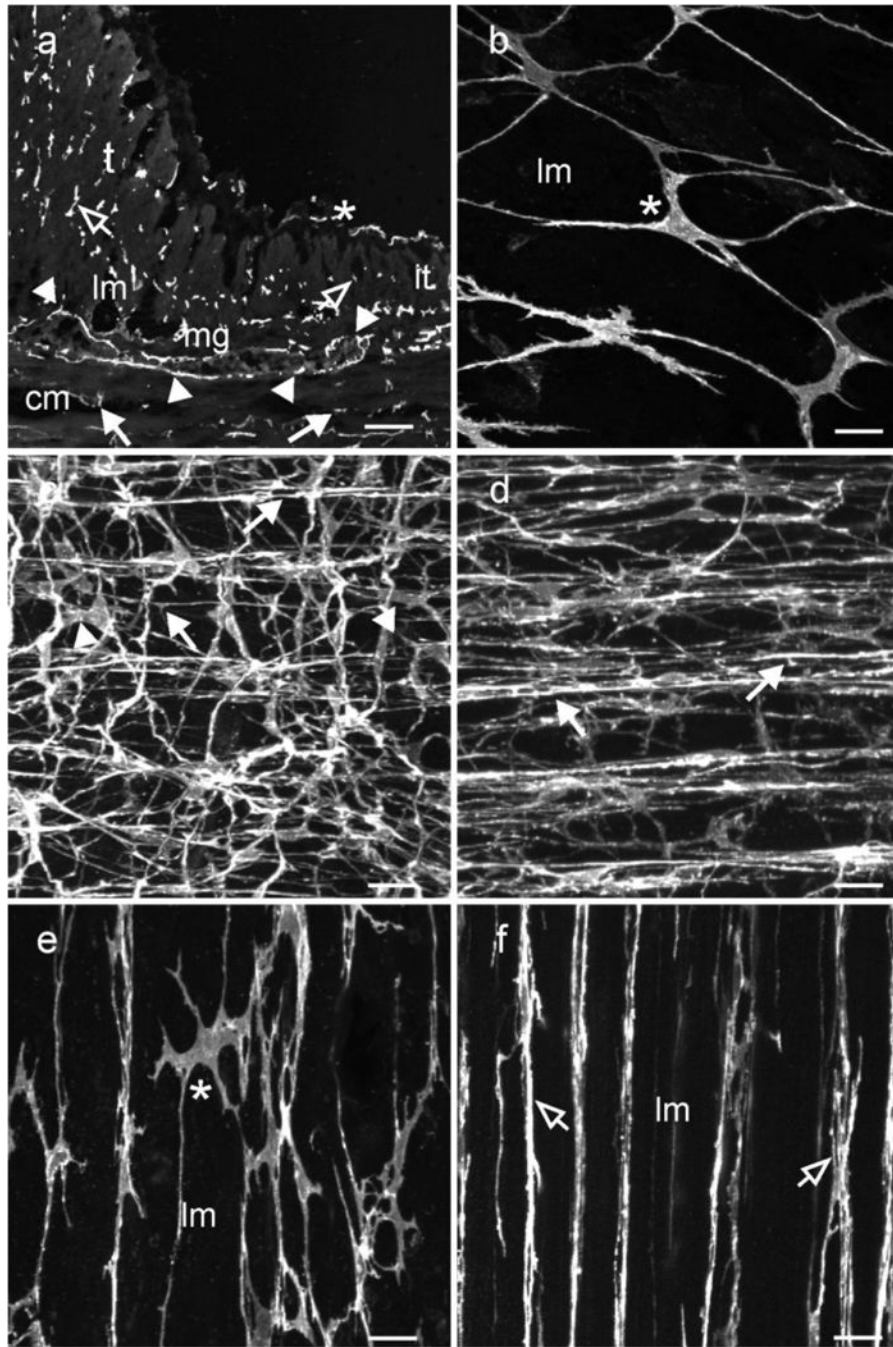


Fig. 4. Distribution of ICC within the proximal colon. Kit^+ ICC were distributed at several anatomical locations within the colonic wall and their density differed in taenia versus intertaenia regions. **(a)** shows a cryostat section through a region of the colonic wall containing intertaenia (it) and a more pronounced taenia (t) muscle. ICC-MY (arrowheads) can be seen surrounding a myenteric ganglia (mg), located between the circular (cm) and longitudinal muscle (lm) layers. ICC-IM are present within the circular (solid arrows) and longitudinal muscle layers (open arrows). **(b-d)** show whole mounts of Kit^+ ICC along the serosal

surface (**a,b,e**; *) of an inter-taenia region forming a loose interconnecting network and ICC-MY at the level of the myenteric plexus forming a dense anastomosing network (arrowheads; **c**). The processes that extended from a triangular or oval perinuclear region often bifurcated into multiple processes and contacted adjacent ICC-MY. (**d**) Shows a dense population of ICC-IM within the circular muscle layer. ICC-IM appeared to form rope-like networks, processes extended from the main axis of ICC-IM to connect with adjacent ICC-IM. ICC-IM were also observed within the longitudinal muscle layer where they ran parallel to smooth muscle cells. (**e,f**) reveal several distinct populations of ICC within the taenia. Panel (**e**) shows ICC-SS in the taenia that formed a loose interconnecting network (*). The main axis of these cells ran parallel with the longitudinal muscle cells and lateral projections contacted adjacent ICC forming an interconnecting network. (**f**) shows a second population of ICC within taenia. This population of ICC-IM was spindle shaped, were distributed throughout the band of muscle and ran parallel to the smooth muscle cells. ICC-IM did not possess the numerous lateral projections seen in ICC along the serosal surface. Scale bars = 100 μm in (**a**) and 25 μm in (**b,c,d,e & f**)

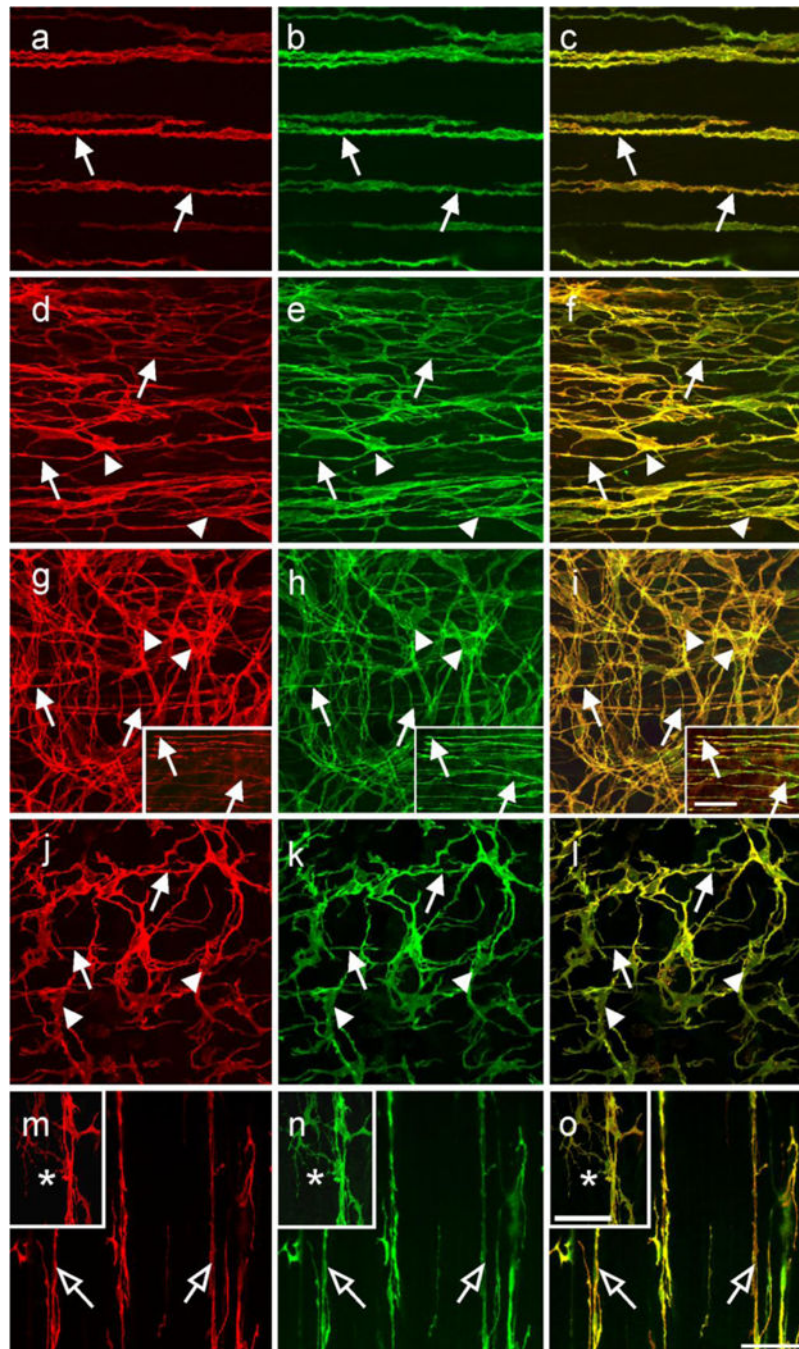


Fig. 5. Cellular co-localization of Kit and ANO1/TMEM16A in ICC throughout the monkey GI tract. (a–c) show Kit (a; red) and TMEM16A (b; green) in ICC-IM (arrows) of the gastric fundus circular muscle. (c) shows a digital overlay of panels (a,b). Both Kit and ANO1 were co-localized in ICC-IM (arrows, yellow). (d–f) show Kit (d; red) and ANO1 (e; green) in ICC-IM (arrows) and ICC-MY (arrow heads) within the gastric antrum. Both Kit and ANO1 were co-localized within both populations of ICC (f; yellow). (g–i) show Kit (g; red) and ANO1 (h; green) in ICC at the level of the deep muscular plexus (ICC-DMP; arrows) and

ICC-MY (arrowheads) of the small intestine. Digital overlay of **(g,h)** is shown in **(i)**. Kit and ANO1 were co-localized in both ICC-DMP and ICC-MY (**i**; yellow) in the small intestine. Digital images of Kit and ANO1 labeling within ICC-DMP and their co-localization are shown in the insets of panels **(g-i)** (arrows). **(j,k)** show Kit (**j**; red) and ANO1 (**k**; green) labeling in ICC-IM (arrows) and ICC-MY (arrowheads) within the proximal colon. Co-localization of Kit and ANO1 is shown in **(l)**; yellow). Panels **(m-o)** show Kit and ANO1-LI cellular co-localization in different populations of ICC of the taenia. Intramuscular ICC (open arrows) were both Kit (**m**; red) and ANO1 (**n**; green) immunopositive (as shown in the digital overlay in panel **o**). Serosal ICC (*) in the taenia were also Kit and ANO1⁺ (**m-o**, insets). Scale bar in **(o)** = 50 μm and applies to all panels. Scale bar in the inset in **(i)** = 50 μm and applies to insets in **(g-i)**. Scale bar in inset in **(o)** = 50 μm and applies to insets in **(m-o)**

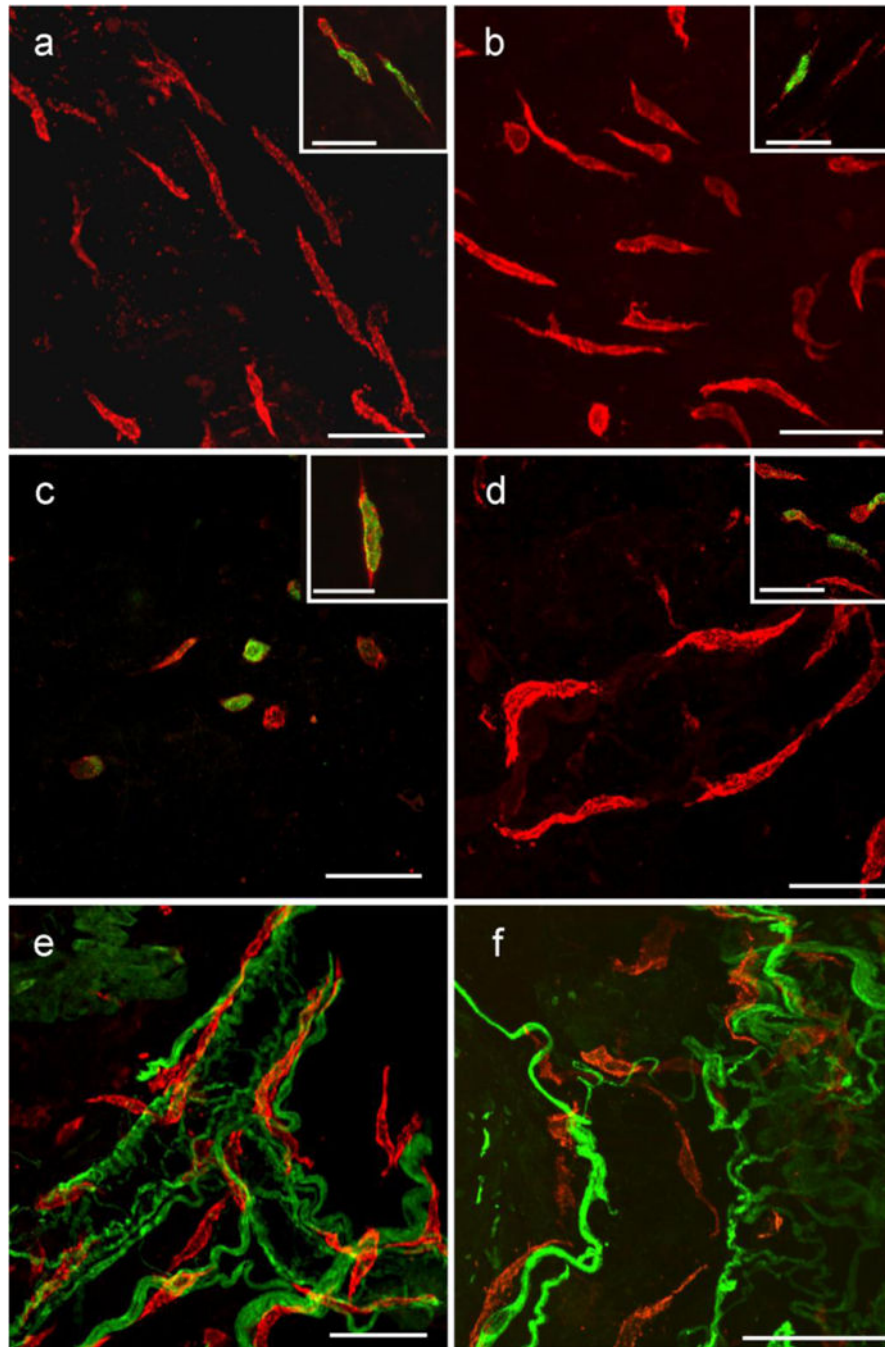


Fig. 6. Kit⁺ cells within the submucosa and lamina propria of the GI tract. Flat sections and whole mount preparations of the mucosa and underlying submucosa from stomach, small intestine and colon. Kit⁺ cells within the submucosa and lamina propria in the gastric fundus (**a**), antrum (**b**), small intestine (**c**) and colon (**d**) were spindle shaped and did not appear to have a distinct orientation except when in close association with submucosal blood vessels (**e,f** colon shown). In the small intestine the number of these Kit⁺ cells that were spindle shaped was less than in other organs, but a larger number of rounded Kit⁺ cells were observed in the

intestinal submucosa. Double labeling with PGP 9.5 and Kit revealed that the spindle shaped cells ran close to but were not intimately associated with nerves. PGP 9.5 labeling also identified autonomic nerves associated with submucosal blood vessels and spindle shaped cells were closely associated with these vessels (**e**). Double labeling with Kit and histamine revealed a sub-population of these spindle shaped cells were histamine⁺ in the stomach, small intestine and colon, suggesting these cells were likely mast cells (insets in **a–d**). Scale bar in (**o**) = 50 μm and applies to all panels. Scale bar in the inset in (**i**) = 50 μm and applies to insets in (**g–i**). Scale bar in all panels and insets = 50 μm , except inset in (**c**) = 25 μm

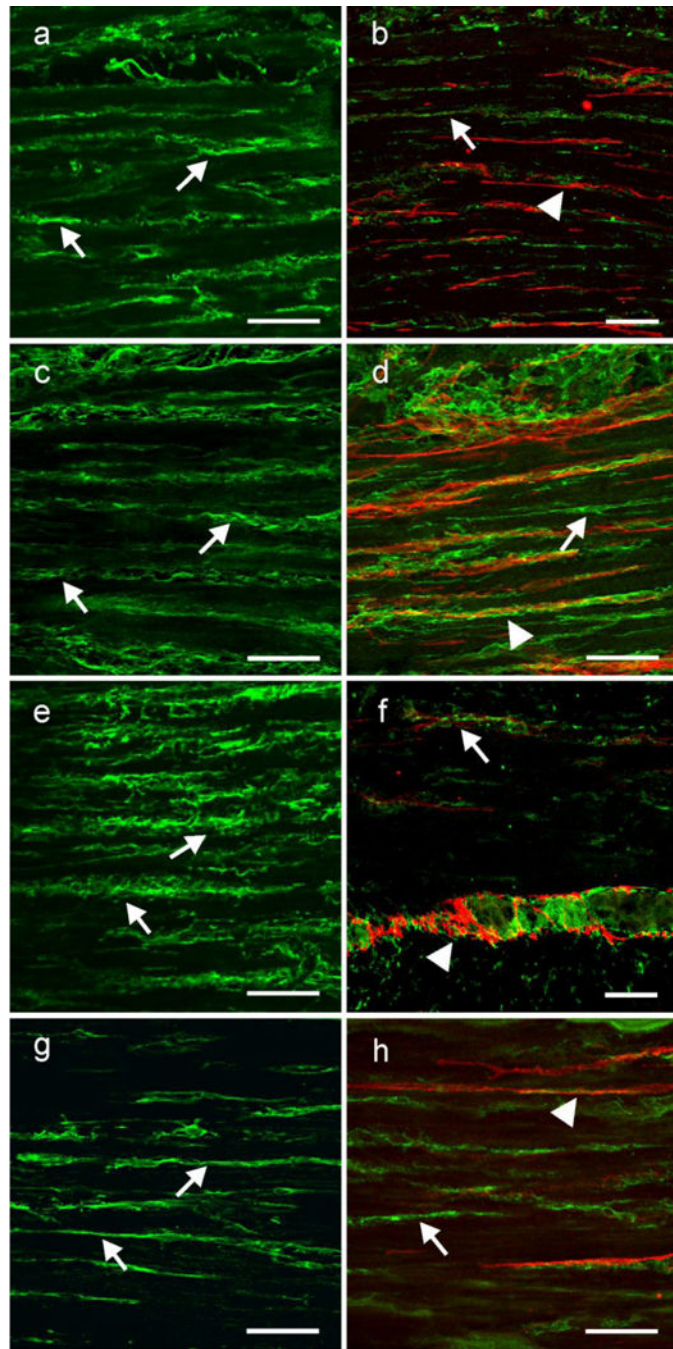


Fig. 7. PDGFR α is expressed in a separate population of interstitial cells that are not Kit $^+$. **(a,c,e,g)** Shows the cellular distribution of PDGFR α within the circular muscle layer of the gastric fundus, antrum small intestine and colon, respectively. PDGFR α $^+$ cells (arrows) ran parallel to the long axis of the circular muscle fibers. **(b,d,f,h)** show double labeling of PDGFR α (green; arrows) and Kit (red; arrow heads) in two populations of cells in the fundus, antrum, small intestine and colon, respectively. Although the two cell populations were closely

apposed to one another they were distinct, providing evidence that PDGFR α ⁺ cells were not Kit⁺ ICC. Scale bars in all panels = 50 μ m

Author Manuscript

Author Manuscript

Author Manuscript

Author Manuscript

Table 1

Details of antibody combinations used for double-label immunohistochemistry.

Combined antibodies	Resource	Mono- or poly-clonal antibodies	Host	Dilution
Kit/SP31	R&D Systems Inc., Minneapolis, MN, USA/Abcam, Cambridge, MA, USA	Poly-/Mono-	Goat/Rabbit	1:100/1:800
Kit/histamine	R&D Systems Inc., Minneapolis, MN, USA/Immunostar, Hudson, WI, USA	Poly-/Poly-	Goat/Rabbit	1:100/1:500
Kit/PGP9.5	R&D Systems Inc., Minneapolis, MN, USA/UltraClone Limited, Isle of Wight, England, UK	Poly-/Poly	Goat/Rabbit	1:100/1:2000
Kit/hPDGFR α	Dako North America, Inc. Carpinteria, CA, USA/R&D Systems Inc., Minneapolis, MN, USA	Poly-/Poly-	Rabbit/Goat	1:100/1:100

Note: hSCF-R: anti-human stem cell factor receptor; SP31: anti-anoctamin 1; PGP9.5: anti-protein gene product 9.5; hPDGFR α : anti platelet derived growth factor receptor α .